Dispersion Management Using Betatron Resonances in an Ultracold-Atom Storage Ring

K. W. Murch, K. L. Moore, S. Gupta, and D. M. Stamper-Kurn
Department of Physics, University of California, Berkeley, California 94720, USA
(Received 30 August 2005; published 5 January 2006)

Particles circulating at specific velocities in a storage ring can undergo betatron resonances at which static perturbations of the particles' orbit yield large transverse (betatron) oscillations. We have observed betatron resonances in an ultracold-atom storage ring and found these resonances to cause the near-elimination of the longitudinal dispersion of atomic beams propagating at resonant velocities. This effect can improve atom-interferometric devices. Both the resonant velocities and the resonance strengths were varied by deliberate modifications to the storage ring.

DOI: 10.1103/PhysRevLett.96.013202 PACS numbers: 39.10.+j, 03.75.−b, 29.20.Dh

In circular accelerators and storage rings, the transverse oscillations of guided particles about the closed design orbit are known, for historical reasons [1], as betatron oscillations. While such oscillations can usually be kept small in a well-designed device, large-scale betatron motion can nevertheless be excited resonantly by weak, static perturbations of the beam path if the particle beam propagates at specific velocities. In high-energy devices [2] and in neutron storage rings [3], such betatron resonances cause the particle beam to collide with apertures in the device and be lost.

Today, storage rings, and, potentially, circular accelerators, are being developed for ultracold, electrically neutral atoms [4–7] or molecules [8,9], to be used for precise interferometry using guided matter waves [10], studies of low-energy collisions [11,12], and the manipulation of quantum degenerate matter. That these motivations differ from those for high-energy physics suggests that familiar concepts of accelerator physics be examined in a new light.

Here, we explore betatron resonances in a millimeter-scale storage ring for ultracold atoms with energies of around $k_B \times 100\ \mu$K per atom (100 peV per nucleon), orders of magnitude smaller than those in modern particle physics facilities. The exchange of energy between longitudinal and transverse motion at several betatron resonances is directly observed for Bose-Einstein condensates (BECs) propagating in the ring. This exchange dramatically reduces the longitudinal dispersion of the atomic beam, lowering its longitudinal kinetic temperature to the pK range. Such dispersion management may improve measurements of rotation rates [13–15], fundamental constants [16], and other quantities by atom-interferometric schemes that are sensitive only to longitudinal velocities [17]. Our study emphasizes the conceptual unity among storage rings, and suggests that other concepts of accelerator physics, such as nonlinear resonant beam extraction or Landau damping of modulation instabilities, may also be adapted to the ultralow energy domain.

The storage ring used for this work is a magnetic time-orbiting ring trap for ultracold ^{87}Rb atoms [6] (Fig. 1). Atoms are confined to a circular ring of radius $r = 1.25$ mm in the horizontal plane by a transverse potential that is harmonic for small displacements from the nominal beam orbit. Both frequencies for transverse motion in this potential, i.e., the betatron frequencies for radial (ω_r) and for axial (ω_z) motion, are independently adjusted by varying the time-varying magnetic field $B_{\rm rot}$ used in our trap [18]. For atoms in the $|F = 1, m_F = -1\rangle$ hyperfine ground state used in this work, using $B_{\rm rot}$ between 4.8 and 13 G gives betatron frequencies in the range $2\pi(50–90)$ Hz. This range of $B_{\rm rot}$ varies the maximum height of the trapping potential in the transverse directions in the range of $k_B \times (40–100)\ \mu$K.

Pulsed atomic beams are ''injected'' into the storage ring in two stages. First, a nondegenerate gas of 2×10^7 atoms is loaded in a portion of the storage ring, with an azimuthal confining potential added to the ring by applying a 9 G horizontal magnetic field [6]. This gas is then cooled to produce a BEC of up to 3×10^5 atoms. Second, the BEC is accelerated over 30 ms by changing the horizontal field so as to lower the potential of the trap minimum and advance its position along the ring. By varying settings in this

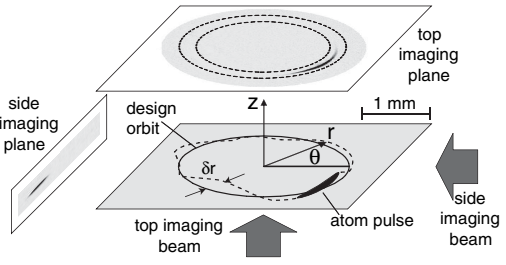

FIG. 1. An ultracold-atom storage ring. Axes are indicated with gravity along $-\hat{z}$. Top or side-view absorption images of the atoms allow their motion to be studied. Dashed circles indicate the 270 μm radial extent of top-view images displayed in polar coordinates as ''annular views'' in Figs. 2 and 4. We refer to motion in r as radial, in z as axial, and in θ as azimuthal or longitudinal. The nominally circular storage ring contains radial δr (exaggerated for illustration) and axial δz beam-path errors and an azimuthal variation $U(\theta)$ in the potential.

acceleration, the mean initial angular velocity of atoms in the ring, Ω_i, is varied between 40 and 120 rad/s [19]. The horizontal field is eliminated over the next 30 ms as $B_{\rm rot}$ is brought to its storage-ring setting.

Important for characterizing betatron motion in a storage ring are the tune parameters, $\nu_{r,z} = \omega_{r,z}/\Omega$, which give the number of betatron oscillations occurring over one complete orbit along the closed-loop beam path. At integer values of the tune parameters, the transverse deflections of particles due to small, spatially fixed perturbations to the beam path accumulate in phase over many orbits to drive large scale betatron motion. This describes a low-order betatron resonance, which is the subject of our work. Higher-order perturbations, such as a modulation of the transverse trapping frequencies or coupling between the two modes of betatron motion, can result in higher-order betatron resonances at noninteger tune parameters and in nonlinear coupling between resonances [2]. We did not observe these higher-order effects in our storage ring.

The propagation of an atomic beam launched at initial velocities either away from or at a betatron resonance is compared in Fig. 2. At the measured axial tune of $\nu_z = 4.2$, the rms azimuthal width of the cloud grows steadily according to an rms azimuthal linear velocity spread of $\Delta v = 1.7$ mm/s [20], equivalent to an rms variation in the tune of $\Delta\nu_z = 6 \times 10^{-2}$, or to a longitudinal kinetic temperature of $T = m(\Delta v)^2/k_B = 28$ nK. At this rate of expansion, the propagating cloud fills a large portion of the storage ring within 10 revolutions.

An atomic beam launched at a resonant tune parameter evolves quite differently. With the mean tune $\nu_z = 4.0$ set to an integer value, about half of the atoms are ''caught'' in a betatron resonance, and their longitudinal dispersion ceases so that a compact portion of the beam remains even after 18 revolutions [Fig. 2(b)]. Starting after about 250 ms, the width of this fraction shows no further growth. Based on measurements from the earliest and latest times in Fig. 2(c), we estimate the rms velocity spread of this portion of the beam to be below 100 μm/s, reducing the range of tunes to $\Delta\nu_z < 4 \times 10^{-3}$. This corresponds to a longitudinal kinetic temperature below 100 pK. To our knowledge, this is the lowest kinetic temperature ever reported for an atomic beam.

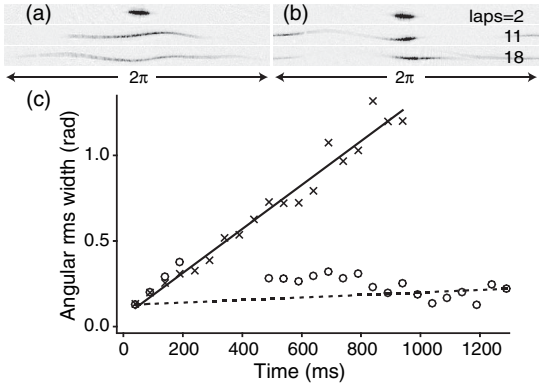

FIG. 2. Dispersion management of matter waves in a storage ring. Annular (top) views are shown after 2, 11, and 18 complete revolutions for initial mean axial tunes of (a) $\nu_z = 4.2$ and (b) $\nu_z = 4.0$. Slight bends in the cloud result from radial betatron motion excited during the injection sequence. (c) The rms width of all (X's for $\nu_z = 4.2$) or just the compact portion (circles for $\nu_z = 4.0$) of the atomic beam is shown vs propagation time, with data for $\nu_z = 4.0$ limited to times when the compact and diffuse portions are separated. A linear fit to data for $\nu_z = 4.2$ (solid line), and a line joining earliest and latest data for $\nu_z = 4.0$ (dashed line) are shown. Here $(\omega_r, \omega_z) = 2\pi(48, 60)$ Hz.

We note that the rms velocity spread of the atomic beam was not directly measured, as could be done, for example, using Doppler-sensitive spectroscopy [21]. Nevertheless, we argue that our estimate for the velocity spread is, indeed, valid, especially in light of the agreement with simulations of the resonance, as described below. An alternative explanation for reduced dispersion due to bright soliton formation [22,23] appears ruled out for two reasons. First, interactions between ^{87}Rb atoms in our ring are repulsive, rather than attractive, while quantum states with a negative effective mass, necessary for the creation of gap solitons [24], do not appear to arise in our storage-ring potential. Second, we also observe a reduced longitudinal dispersion for atomic beams derived from a nondegenerate atomic gas, albeit with greater dispersion than when BECs are launched into the storage ring. These beams have a higher initial kinetic temperature and lower density than those derived from a BEC, conditions that further disfavor soliton formation.

The effects of the betatron resonance are displayed in more detail in Fig. 3. Here, atomic wave packets are launched at tune parameters near $\nu_z = 5$ and then imaged after 640 ms of propagation. The data reveal a stop band [2], i.e., a range of velocities that cannot be maintained in the storage ring. While in a high-energy storage ring particles with velocities within the stop band are lost, in our ring the transverse oscillations at the betatron resonance have energies ($< k_B \times 5$ μK) that are insufficient to expel atoms from the ring. Rather, these atoms accumulate in a narrow range of final velocities at the low-velocity edge of the stop band.

Scanning the beam velocity over a wider range, several betatron resonances can be observed, each yielding a stop band of disallowed velocities (Fig. 4). Resonances are identified as either axial or radial by directly observing the betatron motion. A radial resonance produces an atomic beam that oscillates radially with a phase that differs across the length (i.e., across azimuthal velocities) of the cloud. A side image of the same beam shows no significant axial betatron motion. Conversely, an axial betatron resonance induces axial but not radial oscillations. Such images also confirm that the energy of the atomic beam is conserved at a betatron resonance. For instance,

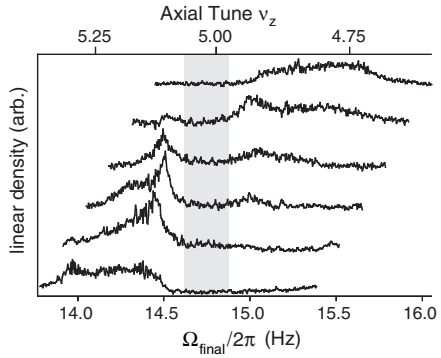

FIG. 3. Matter wave dispersion at an axial betatron resonance. The distribution of final azimuthal velocities is shown for beams with initial mean angular velocities $\Omega_i/2\pi$ evenly spaced between 14.3 (bottom curve) and 15.4 Hz (top curve). Data are offset vertically for clarity. These distributions are obtained from the radially integrated column density of top-view images taken after 640 ms of propagation. Atoms expelled from the stop band (gray shading) accumulate at its low-velocity edge. Since the stop band is narrower than the full initial range of velocities in the beam, only a portion of the beam is affected. Low-velocity atoms for $\Omega_i/2\pi = 14.3$ Hz are affected by the $\nu_r = 5$ radial betatron resonance. Here $(\omega_r, \omega_z) = 2\pi(70, 74)$ Hz.

the 60 μm maximum amplitude of radial betatron motion observed in Fig. 4(a) corresponds to an energy of $k_B \times 3.4$ μK. Given the initial kinetic energy of $k_B \times 62$ μK for atoms launched at $\nu_r = 5$, this motion should reduce the longitudinal velocity by 2.7%, in agreement with the measured magnitude of the stop band.

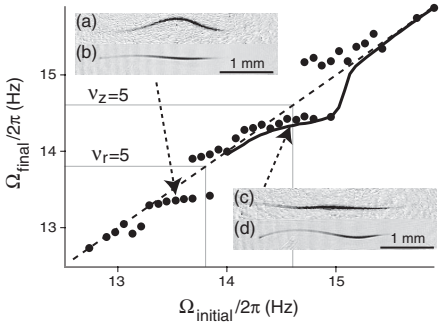

FIG. 4. Stop bands for the $\nu_r = 5$ radial (lower Ω_i) and the $\nu_z = 5$ axial (higher Ω_i) betatron resonances. Mean final angular velocities, determined after 440 ms of propagation in the ring, are shown vs Ω_i. Near the resonances, the atomic beam divides into two portions (Fig. 3), and mean angular velocities of each are given. Simulation results for the axial resonance (solid line), and the relation $\Omega_i = \Omega_f$ (dashed line) are shown. The (a) annular and (b) side views of the atoms launched at $\nu_r = 5$ (radial resonance), and (c) annular and (d) side views of those at $\nu_z = 5$ (axial resonance), show which transverse oscillation is enhanced at each resonance. The horizontal scale for (a) and (c) is chosen to give equal cloud lengths in annular- and side-view images. Here, $(\omega_r, \omega_z)/2\pi = (69, 73)$ Hz.

The atomic beam in these experiments derives from a BEC and is thus characterized by a macroscopic quantum wave function. Away from a resonance, its transverse velocity width is consistent with that of a minimum uncertainty quantum state, as we have determined from its transverse expansion after a sudden release from the storage ring. Nevertheless, since the energy transferred to betatron motion is several hundred times larger than $\hbar\omega_{r,z}$, the relevant harmonic oscillator energy quanta, a purely classical treatment suffices to describe the atomic motion near a resonance.

To model an axial betatron resonance, for example, we consider that the locus of potential minima for our magnetic ring trap deviates from the $z = 0$ horizontal plane by an amount $\delta z(\theta)$. Such a deviation, or beam-path error, arises from imperfections in the electromagnets used to generate the magnetic potential and from stray magnetic fields. Assuming δz is small, the betatron resonance at each integer value of the axial tune arises from beam-path errors with harmonic index $q = \nu_z$ in the Fourier series $\delta z(\theta) = \sum_{q=1}^{\infty} \delta z_q \sin(q\theta + \theta_q)$. The strength of the betatron resonance, given, for example, by the magnitude of the stop band, is then determined by the appropriate magnitude δz_q. Radial betatron resonances, which are caused by radial beam-path errors $\delta r(\theta)$ and azimuthal variations in the potential minimum $U(\theta)$, can be similarly analyzed.

For our simulation, we chose $\delta z = \delta z_5 \sin(5\theta)$ while setting δr and $U(\theta)$ to zero. The magnitude $\delta z_5 = 1.2$ μm was chosen to match the measured magnitude of the resonance stop band (Fig. 4). We then numerically integrated the classical equations of motion for a point particle for 500 ms with the initial condition that the particle propagate purely azimuthally at angular frequency Ω_i with $z = 0$ and radius corresponding to a circular orbit in the absence of beam-path errors. The simulations indicate that for $\omega_z/\Omega_i \simeq 5$, a fraction of the total energy is exchanged between the azimuthal and axial motions, reducing the average longitudinal velocity. The simulations confirm that particles initially propagating at velocities within the stop band are slowed to a narrow range of average velocities, the narrowness of which accounts for the reduced dispersion at the betatron resonance.

The manipulation of matter waves through betatron resonances represents a novel approach to managing dispersion in a circular, multimode atomic waveguide. To make use of such dispersion management (see also Ref. [25]), it is desirable to control both the resonant velocity and also the strength of a betatron resonance. We demonstrate both these capabilities in our storage ring. To vary the betatron resonance frequency, and thereby the resonance velocity, we adjust the transverse trap frequencies in our storage ring. The measured positions of several resonances at various settings of our storage ring,

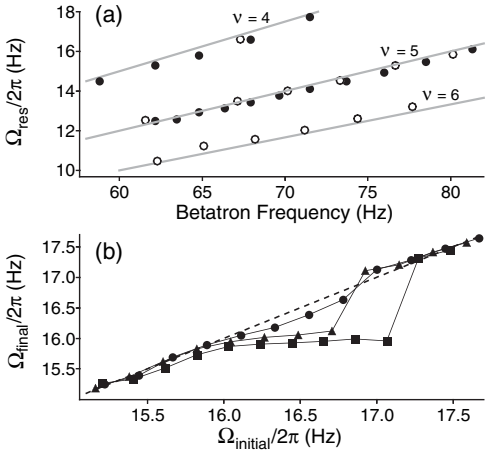

FIG. 5. Tuning the resonant velocities and strength of betatron resonances. (a) Measured angular frequencies Ω_{res} at the low-velocity edge of stop bands observed at several radial (open circles) and axial (filled circles) betatron resonances are shown vs measured betatron frequencies. (b) The $\nu_r = 4$ resonance for $(\omega_r, \omega_z) = 2\pi(68, 74)$ Hz is characterized with a deliberately applied $U(\theta) = U_4 \sin(4\theta)$ azimuthal potential of strength $U_4/k_B = 24$ (circles), 45 (triangles), and 81 nK (squares). The dashed line shows the relation $\Omega_i = \Omega_f$.

shown in Fig. 5(a), exhibit the expected linear scaling of resonant angular velocities with the betatron frequencies. To vary the strength of a specific resonance, we add to our magnetic trap a static radial-quadrupole magnetic field with its axis coinciding with that of the storage ring. This magnetic field adds two types of errors to the ring: a $q = 2$ axial beam-path error and a $q = 4$ potential error $U(\theta)$ proportional to the azimuthal field magnitude (see Ref. [6]). As shown in Fig. 5(b), the strength of the radial betatron resonance at $\nu_r = 4$, assessed by the magnitude of the stop band, is adjusted by varying the magnitude of the deliberately applied $q = 4$ modulation.

Our work may have important implications for guided-atom interferometry. For example, an atom beam produced at an axial betatron resonance will experience less variation in the Coriolis acceleration produced in a frame rotating about the ring axis, as a result of the beam's narrowly defined orbital radius and angular velocity. An atomic Sagnac interferometer [15] could thus detect rotations with higher precision. On the other hand, the excitation of betatron motion [26,27] may add uncertain path-dependent phases in an atom interferometer. The effects of betatron resonances, which cause even small defects in a waveguide to induce large betatron oscillations of guided atoms, will require further scrutiny as guided-atom interferometers are developed and deployed.

We thank J. Wurtele, D. Meschede, and W. Ketterle for helpful comments. This work was supported by DARPA (Contract No. F30602-01-2-0524), and the David and Lucile Packard Foundation. K. L. M. acknowledges support from NSF, and S. G. from the Miller Institute.

[1] D. W. Kerst and R. Serber, Phys. Rev. **60**, 53 (1941).
[2] *CAS-CERN Accelerator School: 5th General Accelerator Physics Course Proceedings*, edited by S. Turner (CERN, Geneva, 1994).
[3] K.-J. Kügler, K. Moritz, W. Paul, and U. Trinks, Nucl. Instrum. Methods **228**, 240 (1985).
[4] J. A. Sauer, M. D. Barrett, and M. S. Chapman, Phys. Rev. Lett. **87**, 270401 (2001).
[5] S. Wu, W. Rooijakkers, P. Striehl, and M. Prentiss, Phys. Rev. A **70**, 013409 (2004).
[6] S. Gupta *et al.*, Phys. Rev. Lett. **95**, 143201 (2005).
[7] A. S. Arnold, C. S. Garvie, and E. Riis, cond-mat/0506142.
[8] F. M. H. Crompvoets, H. L. Bethlem, R. T. Jongma, and G. Meijer, Nature (London) **411**, 174 (2001).
[9] F. M. H. Crompvoets *et al.*, Phys. Rev. A **69**, 063406 (2004).
[10] Y.-J. Wang *et al.*, Phys. Rev. Lett. **94**, 090405 (2005).
[11] C. Buggle, J. Leonard, W. von Klitzing, and J. T. M. Walraven, Phys. Rev. Lett. **93**, 173202 (2004).
[12] N. R. Thomas, N. Kjaergaard, P. S. Julienne, and A. C. Wilson, Phys. Rev. Lett. **93**, 173201 (2004).
[13] F. Riehle *et al.*, Phys. Rev. Lett. **67**, 177 (1991).
[14] A. Lenef *et al.*, Phys. Rev. Lett. **78**, 760 (1997).
[15] T. L. Gustavson, P. Bouyer, and M. A. Kasevich, Phys. Rev. Lett. **78**, 2046 (1997).
[16] D. S. Weiss, B. C. Young, and S. Chu, Phys. Rev. Lett. **70**, 2706 (1993).
[17] P. R. Berman, *Atom Interferometry* (Academic Press, New York, 1996).
[18] The time-varying field, evaluated at a point on the ring, is $B_r \sin(\omega_{\mathrm{rot}} t)\hat{r} + B_z \cos(\omega_{\mathrm{rot}} t)\hat{z}$, with $\omega_{\mathrm{rot}} = 2\pi \times 5$ kHz. Independent control over $\omega_{r,z}$ is obtained by varying B_r and B_z separately. We use the time-averaged magnitude B_{rot} as shorthand. The static transverse gradient at the ring is $B' = 310$ G/cm. See Ref. [6] for details.
[19] A linear relation between Ω_i and the horizontal field used to accelerate the atoms is obtained by measuring beam velocities at several settings far from betatron resonances, and then used to determine Ω_i at all settings. Betatron frequencies are determined by exciting and then observing betatron motion of the propagating atomic beam.
[20] We relate azimuthal linear (v) and angular (Ω) velocities by $v = \Omega r(\Omega)$. To lowest order the change in beam-path radius is $\delta r = \Omega^2 r/\omega_z^2$.
[21] J. Stenger *et al.*, Phys. Rev. Lett. **82**, 4569 (1999).
[22] K. E. Strecker, G. B. Partridge, A. G. Truscott, and R. G. Hulet, Nature (London) **417**, 150 (2002).
[23] L. Khaykovich *et al.*, Science **296**, 1290 (2002).
[24] B. Eiermann *et al.*, Phys. Rev. Lett. **92**, 230401 (2004).
[25] B. Eiermann *et al.*, Phys. Rev. Lett. **91**, 060402 (2003).
[26] A. E. Leanhardt *et al.*, Phys. Rev. Lett. **89**, 040401 (2002).
[27] M. W. J. Bromley and B. D. Esry, Phys. Rev. A **69**, 053620 (2004).